

Effect of molecular weight on craze shape and fracture toughness in polycarbonate

G. L. Pitman and I. M. Ward

Department of Physics, University of Leeds, Leeds, UK
(Received 13 November 1978; revised 26 March 1979)

The shape of the craze at the tip of a crack has been studied using optical microscopy on polycarbonates of various molecular weights at -30°C . For all molecular weights studied the craze shape was well approximated by the Dugdale plastic zone model and this model was used to calculate the craze stress and the release rate in plane strain. It was found that the craze dimensions, the craze stress and the strain energy release rate in plane strain all increased with increasing molecular weight. Fracture of macroscopic specimens showed a mixed mode fracture in all molecular weights. By studying the effect of thickness the strain energy release rate in plane strain was calculated for various molecular weights. Agreement was found between these values and those determined from the craze shape measurements. The overall strain energy release rate, the strain energy release rate in plane strain and the contributions from the plane stress mode increased with increasing molecular weight.

INTRODUCTION

The craze at the crack tip in a glassy polymer was first examined optically by Bessonov and Kuvshinskii¹ and Kambour². Following these earlier studies, we have shown in previous publications³⁻⁵ that the shape of the primary craze can be well approximated by the Dugdale plastic zone model⁶. Recent studies of a similar nature have been undertaken by Döll and Weidmann⁷ and by Vavakin and co-workers⁸. From the Dugdale model it is possible to calculate values of craze stress and fracture toughness from the craze dimensions. It has been shown that the calculated values of fracture toughness for poly(methyl methacrylate) and polycarbonate correlate well with those measured directly in cleavage tests.

The polycarbonate study⁵ revealed a mixed-mode fracture with brittle fracture at the centre and shear lips at the edge of the fracture surface. The results also indicated a possible molecular weight dependence.

The aim of the present investigation is to make a systematic study of molecular weight effects in terms of both craze shape and fracture toughness measurements, and to establish whether the Dugdale plastic zone model can be applied to samples with widely different molecular weights. To obtain a sufficiently wide range of molecular weight electron irradiation⁹ was used.

EXPERIMENTAL

Fracture toughness measurements

The materials primarily used in this investigation were 3 and 6 mm sheets of Lexan polycarbonate and 3 mm sheets of Makrolon 2803 polycarbonate. In addition some results on Lexan rod material and moulded sheets of Makrolon 2400 (similar to those reported in ref 3) were also obtained.

The sheet materials were those from which low molecular weight specimens were prepared by electron irradiation. The molecular weight characteristics of the four basic materials and the irradiated materials are given in *Table 1*. In addition specimens of 4, 5 and 9 mm thickness were prepared, the 4 and 5 mm specimens being milled from the 6 mm Lexan polycarbonate sheets.

Fracture toughness tests were performed using compact tension specimens as shown in *Figure 1*. This fracture toughness test was particularly satisfactory because the electron irradiation method of reducing the molecular weight required a small specimen where the intensity of the electron beam remained fairly constant over the specimen.

Table 1 Molecular weight characterization of polycarbonate samples. FT denotes fracture toughness test undertaken; CS denotes craze shape determined

Sample	\bar{M}_w	\bar{M}_n	Measurements		
Lexan sheet unirradiated	17 900	7150	FT	CS	
	18 000	7000	FT	CS	
	18 100	7200	FT	CS	
	Irradiated	16 300	5000		CS
		16 200	5850	FT	
		16 200	5000		CS
		15 800	5500		CS
		14 900	4950	FT	
		14 800	5100	FT	
		14 700	5000		CS
14 300	4800		CS		
14 100	4700		CS		
12 800	4000		CS		
Makrolon 2803 unirradiated	19 900	8900	FT	CS	
	19 700	8800	FT	CS	
	Irradiated	18 000	7400	FT	CS
16 800		5950	FT	CS	
Lexan rod unirradiated	15 000	4000	FT	CS	
Makrolon 2400 unirradiated	15 000	7900	FT	CS	

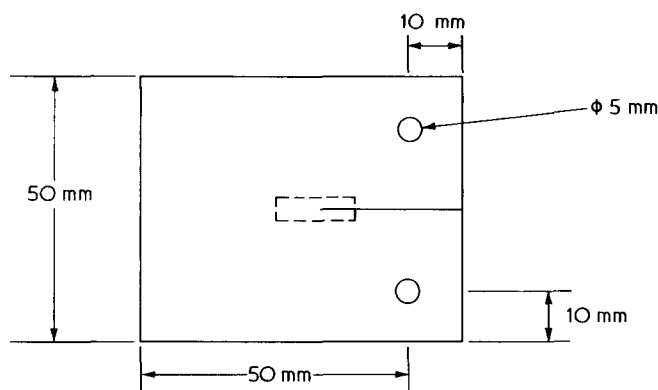


Figure 1 Compact tension specimen geometry

To obtain a sharp crack in the specimen before testing, a fatigue crack was propagated into the specimen at low loads. This was found to be a satisfactory method of pre-cracking for all molecular weights tested.

The fracture tests were performed on an Instron Tensile Testing machine fitted with an environmental chamber. The experiments were carried out at -30°C because at this temperature fracture was by the propagation of a crack through a single craze for all the materials tested. In addition at this temperature the size of the plane stress contribution has been shown to be fairly small^{3,6} permitting a more accurate estimation of the plane strain contribution. Throughout each experiment the temperature was monitored using a thermocouple placed adjacent to the specimen and it was found that the temperature varied by no more than $\pm 1^{\circ}\text{C}$. In all cases a period of at least 1/2 h was allowed between the chamber reaching equilibrium temperature and commencing the test.

The tests were performed at a constant crosshead speed of 0.1 mm min^{-1} , which gave a crack speed of about 2.4 mm min^{-1} . This crack speed allowed stable crack growth for all the materials studied. As the tip of the crack passed lines marked on the specimen, the load and displacement were recorded. In this way it was possible to calculate several results from each specimen.

In addition subsidiary tensile tests were performed at a constant crosshead speed at 5 mm min^{-1} . Specimens were nominally 1 mm thick and 6 mm wide with a gauge length of 30 mm. These tests were performed to study the molecular weight dependence of the extension to break, and so the surfaces of the specimen were polished to remove flaws which can act as stress concentrations.

Measurement of craze shape

The craze shapes were studied by observing the interference fringes produced in reflected light using a Carl Zeiss Jena microscope. In order to obtain the clearest possible fringes light was passed through a filter to give a wavelength of 551 nm. A modified Reichart micro-cold stage was used to obtain the desired temperature (see ref 3 for details). Prior to cooling, the specimen and microscope lens were surrounded with silica gel to reduce condensation on the specimen and the lens.

The specimens for craze observation were made in two ways.

(i) For the tougher higher molecular weight material the craze and crack tip were cut from a compact tension specimen which had previously been used for fracture toughness testing. Figure 2 shows the craze specimen and the angle of

viewing. These specimens were polished for viewing normal to the plane of the crack. They were then placed in the micro-cold stage and returned to the test temperature and wedge loaded.

(ii) It was found that the lower molecular weight material was too brittle to be cut from a compact tension specimen without further crack growth at room temperature. To produce the crack a razor blade was pushed slowly into an uncracked craze shape specimen at the test temperature, causing the crack and craze to propagate ahead of the razor blade.

In both these cases the wedge or razor blade was slowly pushed into the specimen and a series of photographs taken of the fringe pattern until the crack and craze moved forward. The last photograph of the series was considered to be a good approximation to the fringe pattern when the crack starts to propagate. For the smallest crazes (i.e. those with crack opening displacements of less than $5\text{ }\mu\text{m}$) it was found that the positions of the fringe maxima and minima could be found using a microdensometer on the photographic negative. For larger crazes the fringe pattern could not be found using a microdensometer since the variations in the output of the microdensometer were of the same order as the output to the fringes. In these cases the pattern could be resolved from enlarged prints. For the very largest crazes it was found that the best resolution could be obtained by measuring the position of each fringe directly with a vernier eyepiece. Examples of the fringe patterns are shown in Figures 3a and 3b for two different molecular weight polycarbonates. A typical microdensometer trace for a craze in a specimen of molecular weight $\bar{M}_n = 6000$ is shown in Figure 4.

THEORY

Analysis of compact tension specimens

Stress intensity factors for this type of specimen were taken from the calculations of Gross and Srawley¹¹, measuring the load P as the crack passed lines uncracked on the specimen. The modulus was calculated in the manner used by previous workers^{3-5,13}. This analysis assumes that the Irwin-Kies equation¹² is valid, which is only strictly true for linear elastic materials. However, an assessment of the validity of these assumptions can be obtained from the following:

- (i) the plot of load against displacement (Figure 5) for a compact tension specimen is almost linear until crack extension;
- (ii) when unloaded after crack extension the plot is again fairly linear and goes back close to the origin. Figure 6 compares the actual curve with the ideal curve. Crack extension begins at point A, and unloading at point B. The plot returns to C rather than to O which the theory requires. If loading

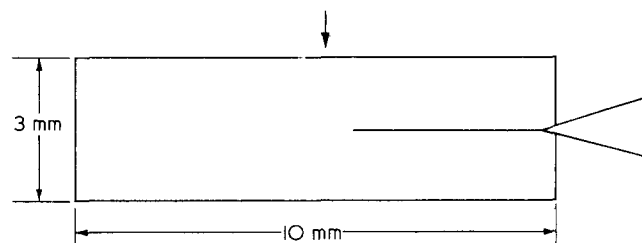


Figure 2 Craze shape specimen geometry. Arrow indicates direction of viewing

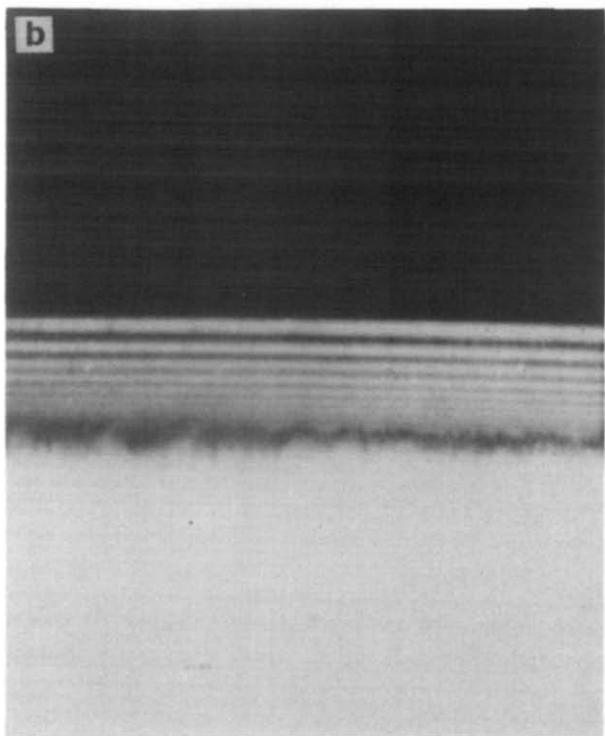
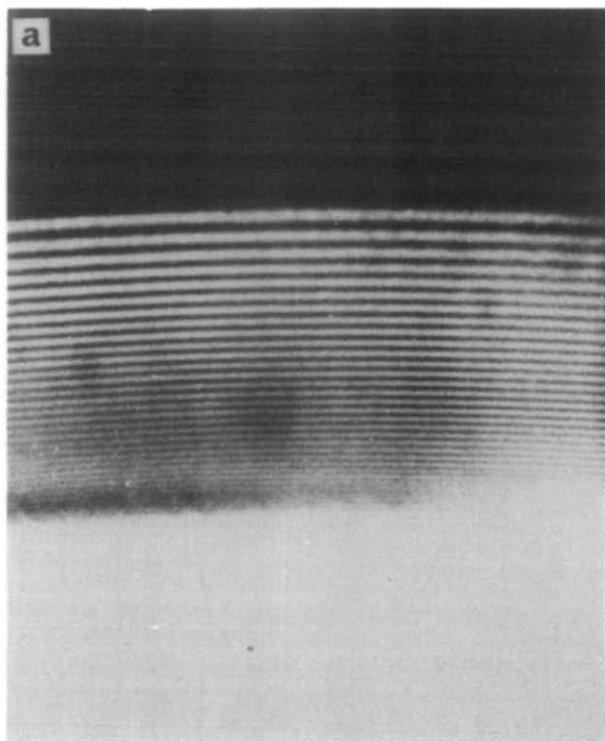


Figure 3 Photographs of interference fringes produced by crazes of molecular weights (a) $\bar{M}_n = 6900, \bar{M}_w = 17500$; (b) $\bar{M}_n = 5000, \bar{M}_w = 15200$

is commenced again further crack growth begins at D. This plot was obtained using the highest molecular weight material tested and thus is the worst case. For lower molecular weight material the loads were lower, which caused fewer inelastic losses and thus an even better fit to the ideal curve.

Dugdale plastic zone model

The Dugdale plastic zone model has been used in previous publications³⁻⁵ to relate craze shape to fracture toughness.

The principal relationships which come from this model were determined by Rice¹⁴, and are:

$$(i) r_c = \frac{\pi}{8} \frac{K_c^2}{\sigma_c^2} \tag{1}$$

where r_c is the craze length, K_c the fracture toughness and σ_c the craze stress.

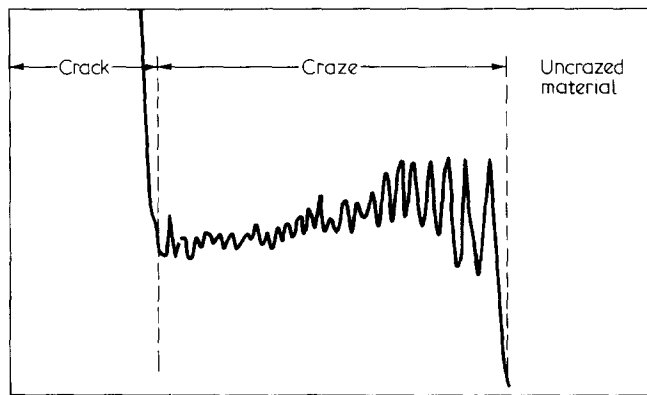


Figure 4 Typical microdensitometer trace of fringes in a polycarbonate craze of molecular weight $\bar{M}_n = 6000, \bar{M}_w = 17000$

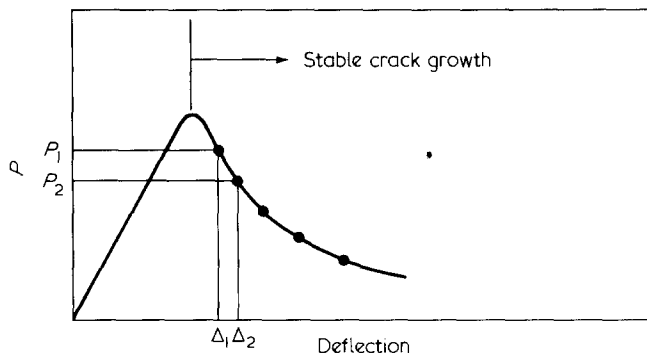


Figure 5 Typical load against deflection curve for a compact tension specimen. The points P_1, Δ_1 and P_2, Δ_2 correspond to the load and deflection for crack lengths a_1 and a_2 , respectively

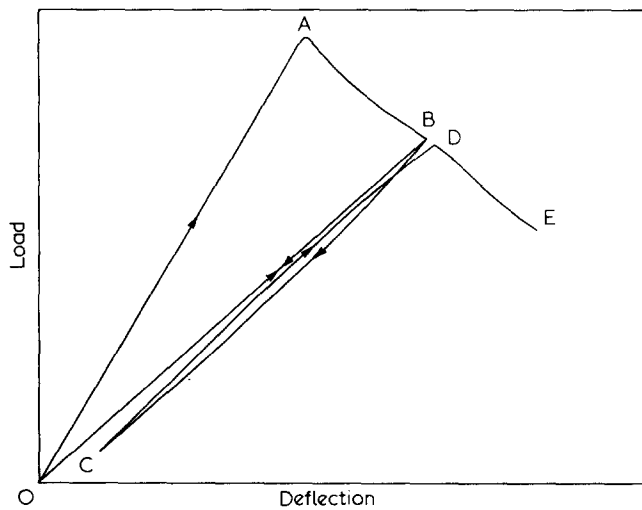


Figure 6 Comparison of ideal load-deflection curve with actual load deflection curve when compact tension specimen is unloaded.

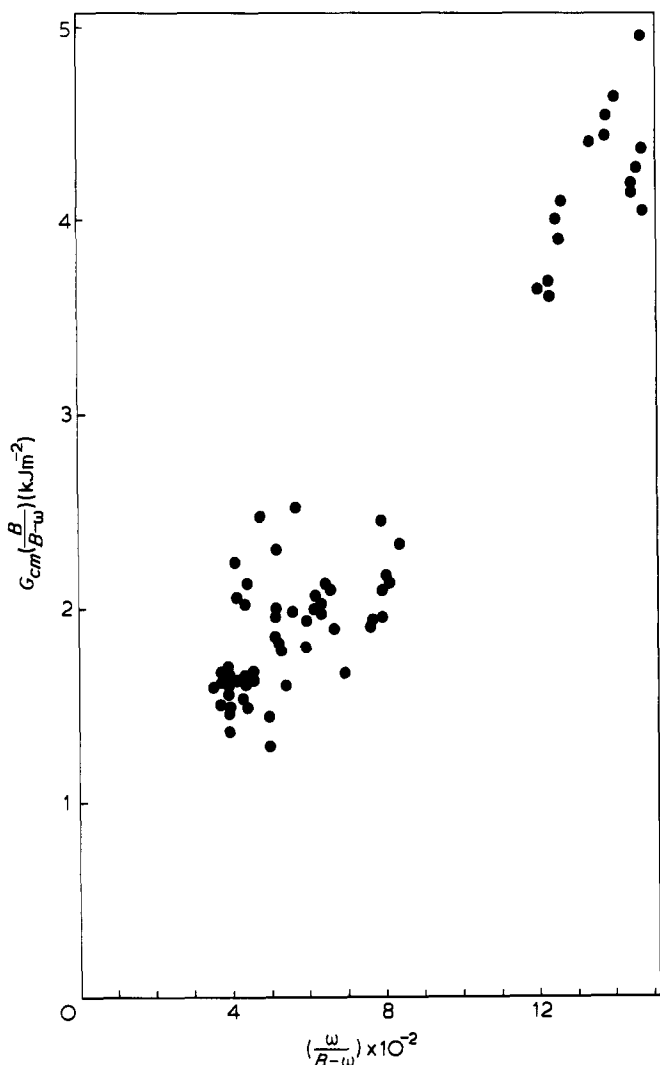


Figure 7 $G_{cm}(B/B - \omega)$ vs. $(\omega/B - \omega)$ for polycarbonate of molecular weight $\bar{M}_n = 7150$; $\bar{M}_w = 18000$

$$(ii) \delta_c = \frac{K_c^2}{\sigma_c E^*} \quad (2)$$

where δ_c is the crack opening displacement, and E^* is the reduced modulus, equal to E for plane stress and $E/(1 - \nu^2)$ for plane stress

$$(iii) \delta(x_1) = \frac{8}{\pi} \frac{\sigma_c r_c}{E^*} \left\{ \xi - \frac{x_1}{2r_c} \log_e \frac{(1 + \xi)}{(1 - \xi)} \right\} \quad (3)$$

where $\delta(x_1)$ is the thickness of the craze at a distance x_1 from the crack tip, and

$$\xi = \left(1 - \frac{x_1}{r_c} \right)^{1/2}$$

RESULTS AND DISCUSSION

Fracture toughness measurements

Mixed mode fracture. The polycarbonate studied in this investigation exhibited mixed mode fracture. Most of the fracture surfaces showed a brittle-type fracture with evidence of crack propagation through a primary craze, while at the edges of the fracture surface ductile shear lips were present.

This is exactly the same situation as that previously presented⁵.

Fraser and Ward⁵ proposed that it is possible to account for this mixed mode fracture by adding the contributions from the plane strain and plane stress regions. The measured strain energy release rate is then given by:

$$G_{cm} = \frac{G_{Ic}(B - \omega)}{B} + G_{IIIc} \frac{\omega}{B} \quad (4)$$

where G_{Ic} is the plane strain value of the strain energy release rate, G_{IIIc} is the plane stress value of the strain energy release rate, B is the specimen thickness and ω the total width of shear lip on the fracture surface. This is a similar approach to that of Parvin and Williams¹⁰ who combined stress intensity factors in the same way.

From equation (4) the plot of $G_{cm}(B/B - \omega)$ against $(\omega/B - \omega)$ would be expected to extrapolate to G_{Ic} as $(\omega/B - \omega)$ tends to zero, while the gradient would give G_{IIIc} . Figure 7 shows such a plot for the unirradiated Lexan sheets with thicknesses from 3 to 6 mm and, although there is a reasonable correlation, the data show a good deal of scatter. This scatter can account for the fact that the value of G_{Ic} of about 0.5 kJm^{-2} is appreciably lower than that calculated from the craze shape (see below). It is proposed that the scatter is because this model does not take into account the form of the shear lips. The shape of the shear lips in a completely fractured specimen is shown in Figure 8a. In most of these tests, in order to look at the craze, the crack was stopped and the specimen unloaded again. This caused the compression of the shear lips and the final shape is shown in Figure 8b. To a first approximation we would expect the energy contribution from the shear lips to be proportional to the volume of yield. Therefore equation (4) can be written as:

$$G_{cm} = G_{Ic} \left(\frac{B - \omega}{B} \right) + \frac{\phi \omega^2}{2B} \quad (5)$$

where ϕ is the energy to fracture unit volume of shear lip. An identical approach proposed by Krafft *et al.*¹⁵ and outlined by Knott¹⁶ has been used to account for shear lips in metals with some success. Figure 9 shows the same data as for Figure 7 but plotted against $\omega^2/B - \omega$. It can be seen that there is a great decrease in scatter and this is reflected in the correlation coefficients of 0.82 for the data plotted on Figure 7 and 0.98 for the data plotted on Figure 9. The extrapolated value of G_{Ic} from Figure 9 is 0.99 kJm^{-2} which is reasonably close to the value calculated from the craze shape. Equation (5) was therefore used to calculate G_{Ic} and ϕ for the different molecular weight materials.

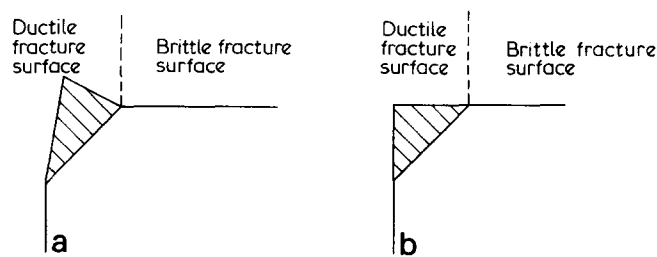


Figure 8 Shape of shear lip (a) in completely fractured specimen; (b) in specimen which has been unloaded

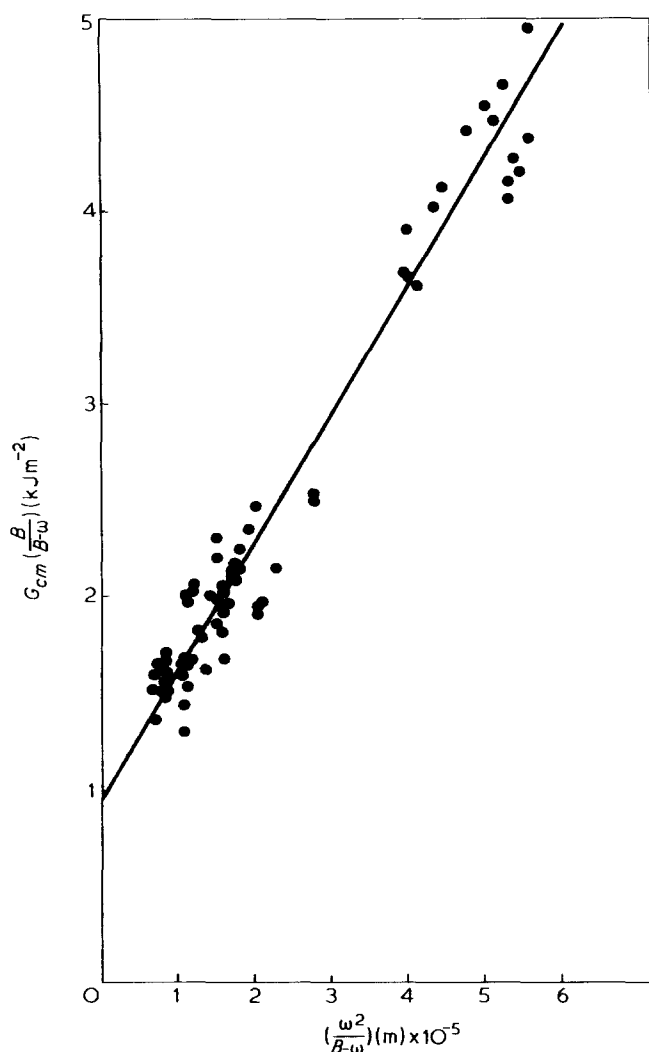


Figure 9 $G_{cm}(B/B - \omega)$ showing some data as in Figure 7

Molecular weight dependence. Figure 10 is an illustration of the importance of molecular weight on the fracture of polycarbonate. In this Figure the overall strain energy release rate, G_{cm} , is plotted against \bar{M}_n for 3 mm thick specimens of Lexan sheet and Makrolon 2803. There was a dramatic increase in G_{cm} between $\bar{M}_n = 5000$ and $\bar{M}_n = 8000$. The corresponding dependence of G_{1c} for the Lexan sheet and ϕ for both the Lexan and Makrolon 2803 specimens are shown in Figures 11 and 12.

Since only 3 mm thick specimens of Makrolon were tested it was not possible to calculate G_{1c} and ϕ directly from the fracture data using equation (5), as this requires more than one value of specimen thickness. However, it is possible to calculate ϕ for Makrolon polycarbonate if it is assumed that the values of G_{1c} calculated from the craze shape are correct (see below). Figure 12 shows values of ϕ for both Lexan and Makrolon estimated on this basis, from which it appears that there was little, if any, dependence of ϕ upon molecular weight within experimental error.

Although ϕ was fairly independent of molecular weight the contribution from the shear lips to the fracture energy increased greatly due to the increase in shear lip width with molecular weight (Figure 13). The edge of the ductile zone marks the point where the stress fields are equally likely to give crazing or yield. Because the stress field required to produce yielding is less dependent on molecular weight than

that required to produce crazing (in simpler terms, the craze stress is more molecular weight dependent than the yield stress) the width of the yielded zone increases with increasing molecular weight.

Tensile tests. From our simple model of shear lip energies we would expect ϕ to be linearly dependent on the total energy to failure in a tensile specimen. Figure 14 shows that there was little increase in the extension to break for \bar{M}_n from 4500 to 7150 in tensile tests at -30°C . Therefore we would expect only a small increase in ϕ over this molecular

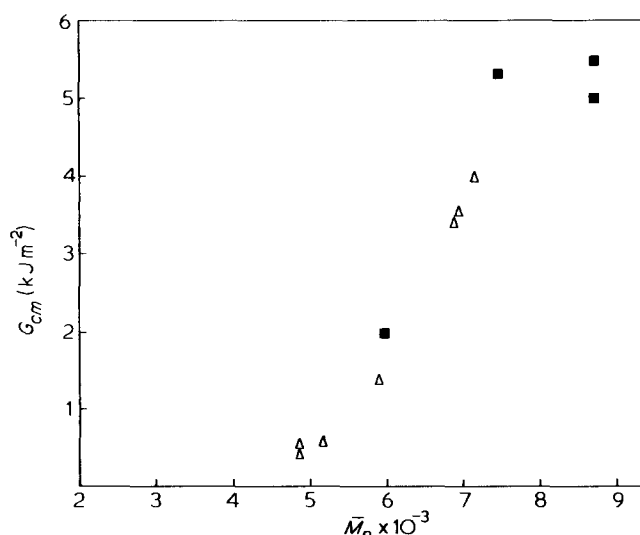


Figure 10 Measured strain energy release rate, G_{cm} vs. number-average molecular weight. Δ , Lexan sheet; \blacksquare , Makrolon 2803

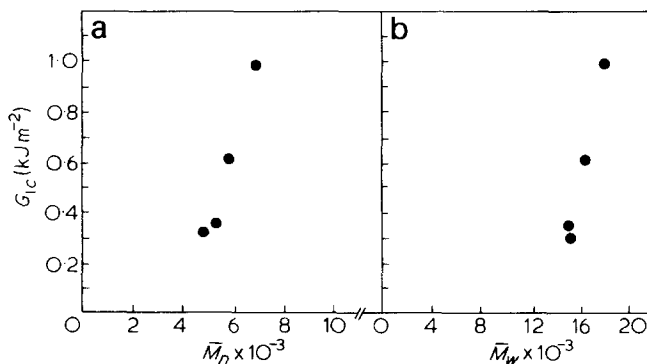


Figure 11 Measured strain energy release rate in plane strain, G_{1c} vs. (a) number-average molecular weight, (b) weight-average molecular weight for Lexan sheet

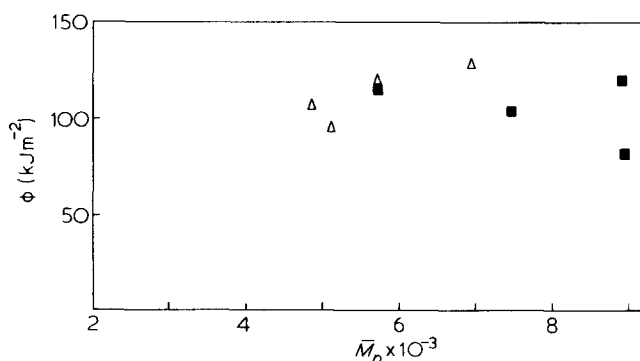


Figure 12 Energy to fracture unit volume of shear lip, ϕ vs number average molecular weight. Δ , Lexan sheet, \blacksquare , Makrolon 2803

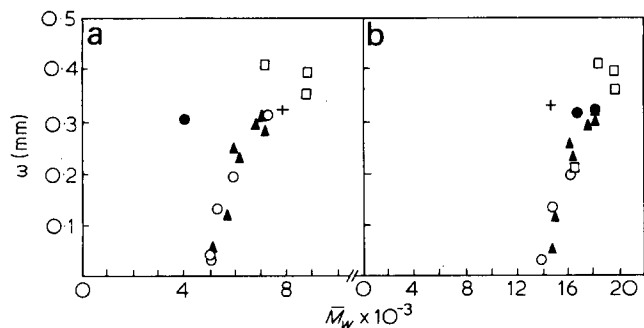


Figure 13 Total width of shear lips, ω vs. (a) number-average molecular weight, (b) weight-average molecular weight. \circ , 3 mm Lexan sheet; \blacktriangle , 6 mm Lexan sheet; \square , Makrolon 2803; \bullet , Lexan rod; $+$, Makrolon 2400

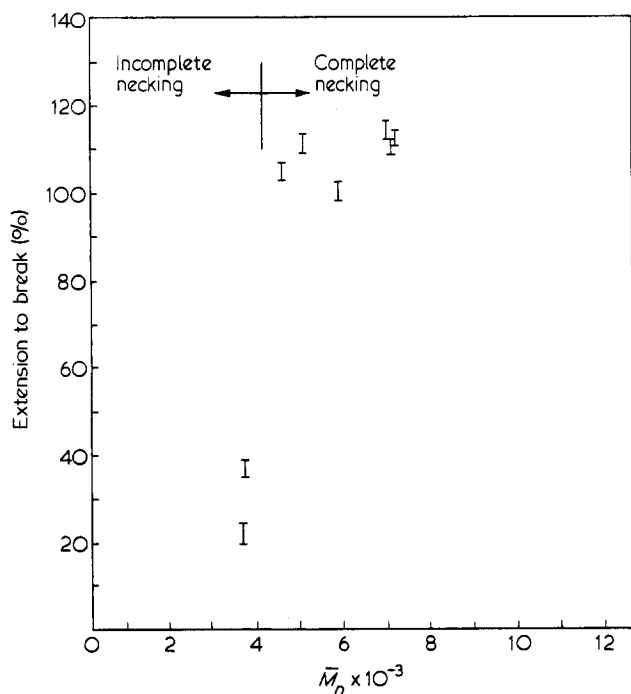


Figure 14 Extension to break vs. number-average molecular weight for Lexan sheet polycarbonate

weight range. The slight increase in extension to break is due to an increase in the amount of strain hardening that the material can perform before fracture. For molecular weights below $\bar{M}_n \approx 4500$ the reduction in strain hardening also caused a reduction in the extent of necking since the neck did not extend the complete gauge length before ductile fracture.

From the value of yield stress in these specimens at -30°C (about 84 MNm^{-2}) and the extension to break it is possible to estimate an approximate value of the energy to fracture unit volume of ductile material. A typical extension of 110% gives an energy of 92 MJm^{-3} . This compares with a typical value of ϕ of 120 MJm^{-3} , which is in reasonable agreement considering the simplicity of the model of shear lips.

Craze shape tests

Use of the Dugdale plastic zone model. Some examples of the interference fringes produced by crazes are shown in Figure 3. The condition for bright fringes is

$$\delta(x_1) = \left(m + \frac{1}{2}\right) \frac{\lambda'}{2} \tag{6}$$

where $m = 0, 1, 2, 3$ etc. and λ' is the wavelength of light within the craze. The length of the craze was found by extrapolating to $\delta(x) = 0$.

To obtain the craze profile it is necessary to know the refractive index of the craze. This was calculated using the analysis of Brown and Ward³. The extension ratio of the craze at break was found to be 1.65 ± 0.04 for Lexan, and 1.58 ± 0.04 for Makrolon and this was found to be constant over the molecular weight range within experimental error. These values are somewhat higher than the value of 1.41 previously⁵ and the reason for this is not known. The refractive index of the craze at break was found to be 1.15 ± 0.03 for Lexan and 1.16 ± 0.03 in Makrolon.

Using these values for μ_B the craze profiles were plotted and some examples of these are shown in Figures 15a and 15b, for two very different molecular weights. On the same Figures are plotted the best fits to the Dugdale plastic zone model to this data using equation (3). There is some difference between the two, but the Dugdale plastic zone model is certainly a good approximation over most of the craze length. We therefore calculated the craze stress and the plane strain value of strain energy release rate using equations (1) and (2) (i.e. taking a value for r_c from the empirical extrapolation of the positions of the fringes, and a value for δ_c from the total number of fringes observed).

Molecular weight dependence of craze shape. The molecular weight dependence of the craze length, crack opening displacement, craze stress and calculated strain energy release rate in plane strain are shown in Figures 16, 17, 18 and 19, respectively, plotted against both \bar{M}_n and \bar{M}_w . There was an extremely sharp increase in each of these with molecular weight. From the data it appears that the dimensions of the craze tend to zero below $\bar{M}_n = 3500$ or $\bar{M}_w = 12000$. Correspondingly, the calculated strain energy release rate also tends to zero for these molecular weights. Below this, even very low loads caused unstable fracture and razor notching was no longer possible. It seems possible that there was a change of fracture mode here since there was no evidence of crazing on the fracture surface (i.e. no surface

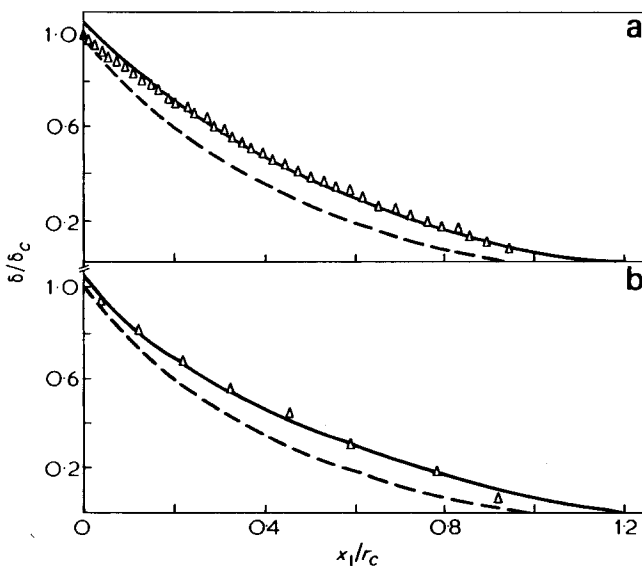


Figure 15 Comparison of craze thickness, δ with Rice equation as a function of distance from the crack tip for (a) $\bar{M}_n = 7150$, $\bar{M}_w = 18000$; (b) $\bar{M}_n = 5000$, $\bar{M}_w = 15200$. \blacktriangle , observed; —, least squares fit; - - - fitted to points 0.1 and 1.0

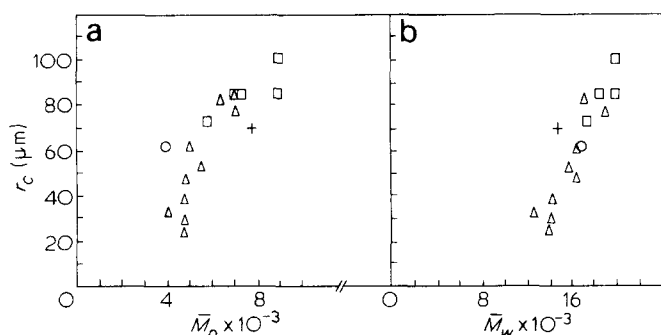


Figure 16 Craze length, r_c vs. (a) number-average molecular weight, (b) weight-average molecular weight. Δ , Lexan sheet; \square , Makrolon 2803; \circ , Lexan rod; $+$, Makrolon 2400

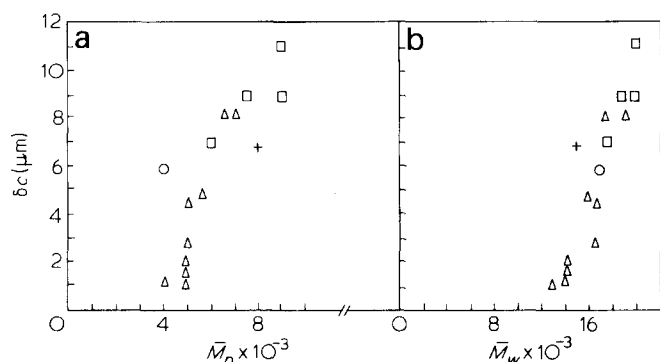


Figure 17 Crack opening displacement, δ_c vs. (a) number-average molecular weight, (b) weight-average molecular weight. Δ , Lexan sheet; \square , Makrolon 2803; \circ , Lexan rod; $+$, Makrolon 2400

colours). A change of fracture mode was identified in PET at low molecular weights by Foot and Ward¹⁷ and Weidmann and Döll showed that the craze dimensions decrease markedly in PMMA at low molecular weights⁷. In a study of the molecular weight dependence of fracture surfaces in PMMA, Kusy and Turner could observe no interference colours, concluding that there was a dramatic decrease in the size of the craze¹⁸.

General considerations

The Dugdale model may well be an oversimplified model compared with the true situation in a polymer. It contains the major assumption that the internal compressive stress is constant along the length of the craze. In addition, we have assumed in our application of the interference method that the refractive index is constant throughout the craze. Despite these possible reservations it can be seen from the results in Figure 19 that the calculated values of G_{1c} agree very well with those measured directly. This confirms that the Dugdale model can be used to obtain estimates of fracture toughness from craze shape observations.

The fracture properties of polycarbonate clearly are strongly dependent on molecular weight. From Figures 13, 16, 17, 18 and 19 it appears that the best correlations are obtained in terms of \bar{M}_w rather than \bar{M}_n . This implies that it is the longer chains that are of most importance in determining the fracture properties.

Kusy and Turner¹⁹ have made a study of the effects of molecular weight on the fracture properties of PMMA and presented a model in which the surface energy measured was determined by the number of chains above a critical length. Their data fitted well with their predictions, reaching a limit

to the surface energy at high molecular weights. However, their analysis does not work well with the data presented here since it fails to predict such a fast dependence upon molecular weight as was observed.

The question of whether the fracture parameters depend on \bar{M}_n or \bar{M}_w , or some other measure of molecular weight, is unresolved. It is hoped that this aspect can be more fully investigated by using materials with a more controlled molecular weight distribution. Such work is now in progress.

CONCLUSIONS

(1) Fracture toughness data for polycarbonates with a wide range of molecular weights were shown to fit a two-mode fracture model, provided that the effect of shear lip size was taken into account. From the results, values for the strain energy release rate in plane strain G_{1c} and ϕ , the energy to fracture unit value of the shear lip, were obtained.

(2) The craze shapes agreed reasonably well with those predicted by the Dugdale plastic zone model. Furthermore there was excellent agreement between the strain energy release rates calculated from the craze shape and the plane strain G_{1c} .

(3) The craze dimensions were very dependent on molecular weight and it was found that this arose from a dependence of both crack opening displacement and craze stress on molecular weight. In addition, although the energy required to produce unit volume of shear lip remained fairly

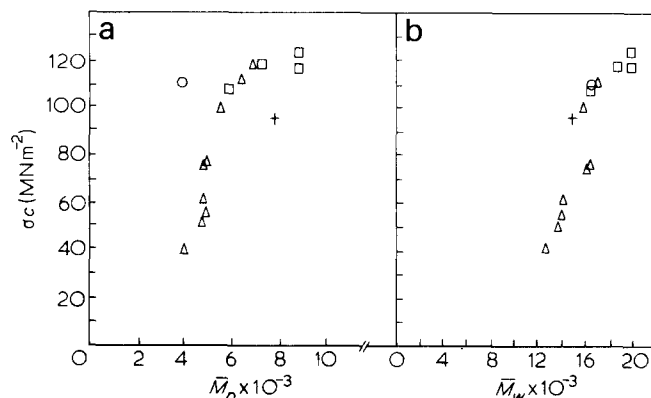


Figure 18 Craze stress, σ_c vs. (a) number average molecular weight, (b) weight average molecular weight. Δ , Lexan, \square , Makrolon 2803, \circ , Lexan rod, $+$, Makrolon 2400

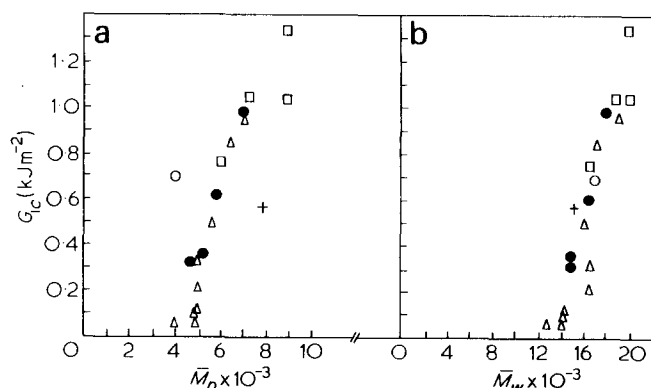


Figure 19 Plane strain strain energy release rate calculated from craze dimensions vs. (a) number average molecular weight, (b) weight average molecular weight. Δ , Lexan sheet, \square , Makrolon 2803, \circ , Lexan rod; $+$, Makrolon 2400; \bullet , measured values taken from Figure 11

constant, the width of the shear lip was highly molecular weight dependent. From these results it follows that both the strain energy release rate in plane strain and the overall measured strain energy release rate were very molecular weight dependent.

ACKNOWLEDGEMENTS

G. L. Pitman was supported on a CASE studentship in collaboration with the Ministry of Defence (PE), PERME, Waltham Abbey. We are grateful to Dr F. Wilkinson of the Cookridge Radiation Laboratory and to Mr S. Hawley of the Polymer Supply and Characterisation Centre, RAPRA for their services of electron beam irradiation and gel permeation chromatography, respectively.

REFERENCES

- 1 Bessonov, M. I. and Kuvshinskii, E. V. *Sov. Phys. (Solid State)* 1961, **3**, 950
- 2 Kambour, R. P. *J. Polym. Sci. (A-2)* 1966, **4**, 349
- 3 Brown, H. R. and Ward, I. M. *Polymer* 1973, **14**, 469
- 4 Morgan, G. P. and Ward, I. M. *Polymer* 1977, **18**, 87
- 5 Fraser, R. A. W. and Ward, I. M. *Polymer* 1978, **19**, 220
- 6 Dugdale, D. S. *J. Mech. Phys. Solids* 1960, **8**, 100
- 7 Döll, W. and Weidmann, G. W. *Colloid Polym. Sci.* 1976, **254**, 205
- 8 Vavakin, S. A., Kozyrev, Yu. I. and Salganik, R. Z. *Izvest. Akad. Nauk SSR, Mekh. Tverd. Tela* 1976, **11**, 111
- 9 Pitman, G. L., Ward, I. M. and Duckett, R. A. *J. Mater. Sci.* 1978, **13**, 2092
- 10 Parvin, M. and Williams, J. G. *J. Mater. Sci.* 1975, **10**, 1883
- 11 Srawley, J. E. and Gross, B. *NASA TNE*, 1967, 5701
- 12 Irwin, G. R. and Kies, J. A. *Welding J. Res. Suppl.* 1954, **33**, 1935
- 13 Brown, H. R. and Ward, I. M. *J. Mater. Sci.* 1973, **8**, 1365
- 14 Rice, J. R. in 'Fracture - An Advanced Treatise', (Ed. H. Liebowitz), Academic Press, New York and London, 1968, Ch 3)
- 15 Krafft, J. M., Sullivan, A. M. and Boyle, R. W. *Proc. Symp. Crack Propagation, Cranfield* 1961, p 8
- 16 Knott, J. F. in 'Fundamentals of Fracture Mechanics', Butterworths, London 1973, p 127
- 17 Foot, J. S. and Ward, I. M. *J. Mater. Sci.* 1972, **7**, 367
- 18 Kusy, R. P. and Turner, D. T. *Polymer* 1977, **18**, 391
- 19 Kusy, R. P. and Turner, D. T. *Polymer* 1976, **17**, 161